Astron. Astrophys. 321, 71–80 (1997)

ASTRONOMY AND ASTROPHYSICS

Depolarization of radio synchrotron emission in spiral galaxies

X. Chi[1,⋆], **E.C.M. Young**[1], **and R. Beck**[2]

[1] Department of Physics and Materials Science, City University of Hong Kong, Tat Chee Avenue, Kowloon, Hong Kong
[2] Max-Planck-Institut für Radioastronomie, Auf dem Hügel 69, D-53121 Bonn, Germany

Received 21 March 1996 / Accepted 23 September 1996

Abstract. The internal depolarization of linearly polarized radio synchrotron emission of spiral galaxies by differential Faraday rotation in regular magnetic fields and by Faraday dispersion in random magnetic fields is formulated in one dimension as a function of radio wavelength λ. The random fields are modeled as a number of cells along the line of sight which obey a Kolmogorov spectrum in size and in field strength and have an isotropic distribution of orientation. A graphic representation of the calculation procedure is introduced for the Faraday dispersion function.

Given a set of typical parameters for spiral galaxies, our model predicts that the fractional polarization is an oscillating function of λ^2 with minima near zero and decreasing amplitude. Compared with single-size cells, the depolarizing effect of the Kolmogorov-type random fields is much smaller; they only smear the effect of the regular field. However, the random fields have a strong effect on the Faraday polarization angle at long wavelengths and distort its linear relation with λ^2. As a result, Faraday rotation measures at decimeter wavelengths oscillate in λ^2 so that their sign may reverse without reversals in the regular magnetic field.

Our model is able to explain observational phenomena like polarized emission around λ90 cm, anomalous variation of depolarization with wavelength, excess rotation measures at λ20 cm, and the lack of a correlation between Faraday rotation measure and depolarization at $\lambda \geq 20$ cm.

Key words: polarization – techniques: polarimetric – radio continuum: galaxies – galaxies: spiral – galaxies: magnetic fields – galaxies: ISM

1. Introduction

Magnetic fields constitute an important component in the interstellar medium of spiral galaxies. Their energy density is generally comparable to those of other components, such as the turbulent motion of gas and cosmic rays. The field strengths are found to be of the order of 10^{-5} Gauss. Although their energy density is too small to assert influence on the rotation of the galactic disk, the galactic magnetic fields are involved in many interstellar processes, ranging from cosmic ray confinement to star formation (see summary by Beck 1987). The popular theory for the origin of the fields is the dynamo amplification in a rotating galactic disk (Ruzmaikin et al. 1988; Wielebinski & Krause 1993; Beck et al. 1996).

In recent years, progress in observational techniques at radio wavelengths has enabled the study of the field structure in nearby spiral galaxies by means of polarized radio continuum emission and internal Faraday rotation measures (Beck 1993; Beck et al. 1996). However, due to the existence of random fields in the host galaxy, the interpretation of polarization data becomes very complicated. For example, the observed distribution of polarization between λ20.5 cm and λ18.0 cm often appears to be "anomalous" in several parts of the spiral galaxy M51, i.e. the fractional polarization at the longer wavelength is larger than that at the shorter one (depolarization $DP > 1$) (Horellou et al. 1992). This phenomenon is difficult to understand because the fractional polarization in random magnetic fields is expected to decrease continuously with increasing wavelength according to the classical formulation by Burn (1966). Further problems with the Burn's model arose in M31 where Faraday depolarization was found not to be correlated with Faraday rotation measures (Berkhuijsen & Beck 1990). Even for radio galaxies, there are also "anomalies" emerging from polarization measurements. Johnson et al. (1995) found that there are "silhouette" strips in the depolarization maps of the radio galaxies 3C34 and 3C340 where depolarization between 6 cm and 20 cm is strong and Faraday rotation measures are very small.

Since the classical work of Burn (1966), most of the theoretical depolarization models of differential Faraday rotation and Faraday dispersion have been made for spherical compact radio sources and radio jets (e.g. Burch 1979; Cioffi & Jones 1980; Laing 1981; Spangler 1983), but little has been done for the extended sources configured as spiral galaxies. Burn's slab model allows analytical calculation of estimates for Faraday depolarization analytically only for the case of a spatially uniform

Send offprint requests to: R. Beck: rbeck@mpifr-bonn.mpg.de
⋆ Now at Dept. of Computer Science, Vanderbilt University, Nashville TN37235, USA

mixture of the regular and random magnetic fields, but not for the (more realistic) case of a non-uniform mixture of these two field components. Furthermore, Burn described the random fields as a large number of small single-size cells along the line of sight and assumed that their Faraday rotation measures obey a Gaussian distribution. The resultant fractional polarization decreases with wavelength as an exponential function of $-\lambda^4$.

Cioffi & Jones (1980) considered the effects of angular resolution of the telescope beam and the inhomogeneity in emissivity and Faraday dispersion. Their formulation is for the regular magnetic field in spherically symmetric sources where the Faraday dispersion is assumed to be internal. Tribble (1991) studied the depolarization of polarized radio flux by an irregular foreground Faraday screen for uniform and linear geometries. Like Burn (1966), he assumed that the rotation measure produced by random fields obeys a Gaussian distribution. Unlike Burn, he argued that the theoretical mean value of the fractional polarization drops faster than observed, which results in an underestimate of the long-wavelength polarization. As observations yield the length of the polarization vector, Tribble argued that the root-mean-square value of fractional polarization should be used for the interpretation of data. All the above results are not suitable for the case of spiral galaxies where the random field scale is finite and the number of random field cells is small.

Finally, Burn's study on Faraday dispersion assumes that all cells have the same size and contain fields of the same strength and plasma with the same electron density, while the propagation of radio waves through the interstellar medium of our Galaxy indicates a power-law distribution in electron density (Rickett 1990), generally described by a Kolmogorov law.

In this work, we expand the basic concept of Burn and formulate the effect of depolarization in Kolmogorov-type random fields. Possible deviations from the Kolmogorov law (Cordes et al. 1985; Malofeev et al. 1996) are not significant for this study. The spatial scale referred there is only $10^9 - 10^{11}$ cm and the effect on Faraday dispersion will be smoothed out.

2. The formulation

2.1. General remarks

Following the notation of Burn (1966), we define the complex linear polarization $P = pe^{2i\chi}$, where p is the fractional polarization and χ is the polarization angle. χ has a linear dependence on λ^2, the wavelength square of the radiation in a uniform magnetic field,

$$\chi(\mathbf{r}, \lambda) = \chi_0(\mathbf{r}) + \phi(\mathbf{r})\lambda^2 \tag{1}$$

where $\mathbf{r}$ is the positional vector from the observer to the source and $\chi_0(\mathbf{r})$ is the intrinsic polarization angle. $\phi(\mathbf{r})$ is the rotation measure and is defined by

$$\phi(\mathbf{r}) = K \int_0^{r_0} n_\mathrm{e}\mathbf{B} \cdot d\mathbf{r} \tag{2}$$

where n_e is the thermal electron density, $\mathbf{B}$ is the magnetic field vector, and K is a constant, $K = 2.62 \times 10^{-17}$ in c.g.s. units. $\phi\lambda^2$ is usually called the Faraday depth. We note that this definition is slightly different from Burn's.

For extended sources configured as spiral galaxies, the polarization of the integrated emission (along the line of sight) is

$$P(\lambda^2) = \int \epsilon(\mathbf{r}, \lambda) p_i(\mathbf{r}) e^{2i[\chi_0(\mathbf{r}) + \phi(\mathbf{r})\lambda^2]} dr \tag{3}$$

where ϵ is the normalized emissivity. If the radiation is synchrotron emission by relativistic electrons with a power-law spectral index γ, the intrinsic fractional polarization is given by $p_i = (\gamma + 3)/(\gamma + 7)$ (e.g. Le Roux 1961). Here γ may be a function of r and so may be p_i.

In our model, it is assumed that the intrinsic polarization angle is constant at different Faraday depths ($\chi_0(\phi)$ = const) and is usually set to zero. The justification for this assumption has been made by Burn (1966) and he gave three examples where the assumption is valid. For the application in our work, since the beam size effect is neglected and the formulation is one-dimensional, we have satisfied the conditions that either the direction of the magnetic field is the same for all parts of the source (Example 1) or the field of the source has random variations around a mean direction (Example 2) if the radiation is assumed to be produced in the mean field.

For simplicity, we assume that the polarized radio synchrotron emission comes only from regions with regular magnetic fields and no emission emerges from cells with random field. This means that we disregard the effect of statistical depolarization by synchrotron emission from cells containing fields with random orientations of their polarization angles. This would reduce the intrinsic fractional polarization p_i by a factor independent of wavelength. This factor depends on the ratio between the energy densities of the regular and the random fields and can be determined from observations at small wavelengths where Faraday effects are negligible (see Table 3 in Buczilowski & Beck 1991).

2.2. Depolarization in single-size cells with random magnetic fields

We start the formulation of the depolarization effect of random fields by Faraday rotation with the single-size cell model. In this model we consider a number of random field cells placed along the line of sight, while the polarized emission emerging from behind the cells.

Let us define the linear size of the cells l_0, and a constant strength of the magnetic field B_R over the scale length l_0. Assuming that the angle between the magnetic field and the observer is θ, we have a Faraday rotation measure for a single cell of

$$\varphi = K n_\mathrm{e} l_0 B_\mathrm{R} \cos\theta \tag{4}$$

Since n_e, l_0 and B_R are constant, the distribution of φ is the same as that of $\cos\theta$. In the case of isotropic orientation in 3-dimensional space, the probability element dF is proportional

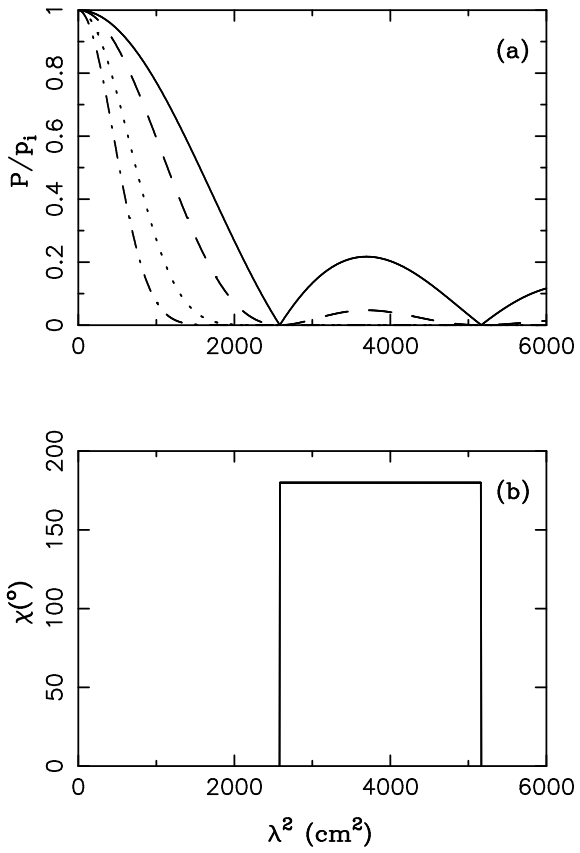

Fig. 1a and b. Depolarization of radio synchrotron emission by a number of single-size cells with random galactic magnetic fields as a function of λ^2. The parameters of each cell are set constant and to typical values: l_0 = 50 pc, n_e = 0.03 cm^{-3} and B_R = 5 μG. Different curves represent cases of a different number m of cells along the line of sight; the solid curve for m = 1; the dashed curve for m = 2, the dotted curve for m = 5 and the dashed-dotted curve for m = 10. **a** The fractional polarization; **b** the polarization angle. Note that it remains zero for even m and flips between 0° and 180° for odd m (which cannot be distinguished observationally).

to the solid angle element $\sin\theta d\theta = -d\cos\theta$. If the probability density f is taken to be an explicit function of $\cos\theta$, $f = dF/d\cos\theta$ becomes a constant. In other words, the distribution of $\cos\theta$ for a cell is uniform over its variation range $[-1, 1]$.

Here we define the Faraday dispersion as the distribution function of Faraday rotation measure at a certain geometrical depth. Then the Faraday dispersion function (normalized probability density) of a random field cell is given by

$$f(\varphi) = \frac{1}{2\varphi_0}, \quad -\varphi_0 \le \varphi \le \varphi_0 \tag{5}$$

with $\varphi_0 = n_e l_0 B_R$. It has the mean $<\varphi>= 0$ and the variance $<\varphi^2>= \varphi_0^2/3$.

When there are m cells along the line of sight, the total rotation measure is the sum of the rotation measures of the individual cells, i.e. $\varphi = \varphi_1 + \varphi_2 + ... + \varphi_m$. Its distribution function or the Faraday dispersion can be calculated by using the characteristic function method. The characteristic function of Faraday dispersion of a single cell $g(t)$ is the Fourier transform of $f(\varphi_j)$,

$$g_j(t) = \int_{-\infty}^{\infty} f(\varphi_j) e^{it\varphi_j} d\varphi_j = \frac{\sin\varphi_0 t}{\varphi_0 t} \tag{6}$$

Then, the characteristic function of φ is

$$G_m(t) = g_1(t)g_2(t)...g_m(t) = \left(\frac{\sin\varphi_0 t}{\varphi_0 t}\right)^m \tag{7}$$

and the Faraday dispersion function can be derived by inversing the Fourier transform

$$\begin{aligned} F(\varphi) &= \frac{1}{2\pi}\int_{-\infty}^{\infty}\left(\frac{\sin\varphi_0 t}{\varphi_0 t}\right)^m e^{-i\varphi t} dt \\ &= \frac{1}{\pi}\int_{-\infty}^{\infty}\left(\frac{\sin 2\varphi_0 t}{2\varphi_0 t}\right)^m e^{-i2\varphi t} dt \end{aligned} \tag{8}$$

The last expression is written in Burn's notation.

With the above Faraday dispersion function, the fractional polarization for radio emission passing through m cells can be written as

$$P(\lambda^2)/p_i = \int_{-\infty}^{\infty} F(\varphi) e^{2i\varphi\lambda^2} d\varphi = \left(\frac{\sin 2\varphi_0\lambda^2}{2\varphi_0\lambda^2}\right)^m \tag{9}$$

where p_i is the intrinsic polarization which is observable at small wavelengths. The imaginary part of the fractional polarization is zero in Eq. (9). This means that the polarization angle is either 0° or 180° (which cannot be distinguished observationally). There is a difference in the period of the polarization curve between our single-size cell model and the slab model of Burn (1966). The period in λ^2 in our formulation is half of that in Burn's. The reason is that our Faraday dispersion function extends over twice the range as Burn's.

Fig. 1 displays the polarization curves for a number of cells m =1, 2, 5, 10, each with typical parameters n_e = 0.03 cm^{-3}, B_R = 5 μG and l_0 = 50 pc. The zero points occur at multiples of $\lambda^2 \simeq 2600$ cm^2. Most polarization observations refer to wavelengths between λ3 cm and 20 cm where the first part of the curve is relevant. The decreasing trend in this part is similar to the Burn's exponential function of $-\lambda^4$ although there is some difference in the rate of decrease. For the case m = 1, the polarization profile is similar to that from Burn's slab model with a regular field.

Fig. 1a shows that the zero fractional polarization points do not change with m, as they only depend on the maximum rotation measure of one single cell, but the amplitude of the fractional polarization decreases with increasing m. When m becomes very large, the amplitude will approach zero. This result is consistent with the argument of Tribble (1991). For even number of m, the polarization angle keeps zero all the way; but for odd number of m, it flips between 0° and 180°. The mean Faraday rotation measure is always zero.

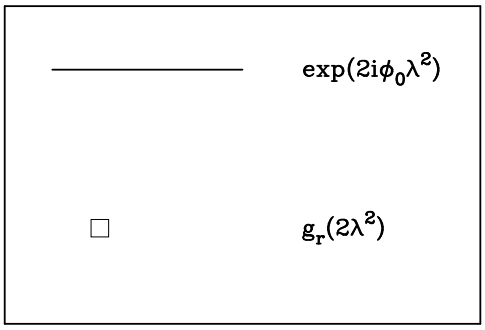

Fig. 2. Graphic representation of the calculation procedure of the Faraday dispersion factors defined in the text. The straight line is for regular magnetic field and the box is for one cell of random magnetic field.

2.3. Depolarization in random and regular fields

Now we combine the Faraday rotation effect of the regular magnetic field with the Faraday dispersion effect of random fields in our formulation. The regular field through geometrical depth x produces a rotation measure

$$\phi_0(x) = K n_{\rm e} B_{\parallel} x \tag{10}$$

where $B_{\parallel}$ is the component of the regular field along the line of sight and here is taken to be constant. Hereafter when referring to the regular field strength in this paper, it means its parallel component. $n_{\rm e}$ is the thermal electron density and is taken to be the same value as that in the cells of random fields. The contribution to the Faraday dispersion function can be represented by a factor

$$G_{\rm u} = e^{2i\phi_0\lambda^2} \tag{11}$$

where λ is the wavelength.

In a similar way, a cell of random field contributes a factor which is just its characteristic function of Faraday dispersion in term of $2\lambda^2$,

$$g_{\rm r} = g(2\lambda^2) \tag{12}$$

where the function form of $g(\lambda^2)$ depends on the properties of the random field and can be derived as Eq. (6) for the single-size cell model. We call $G_{\rm u}$ and $g_{\rm r}$ *dispersion factors*.

In analogy to the Feynman Diagrams (Feynman & Hibbs 1965), we introduce a graphic representation of our calculation procedure of the Faraday dispersion function. $G_{\rm u}$ is represented by a straight line and $g_{\rm r}$ by a box, as shown in Fig. 2. When the linearly polarized radio emission passing through a regular field and m cells of random field, we represent the situation by drawing a straight line first and then drawing m boxes on the line. The total dispersion factor is calculated as the product of all contributing dispersion factors, and the Faraday dispersion function is the Fourier inverse of it

$$F(\phi) = \frac{1}{\pi}\int_{-\infty}^{\infty} [g_{\rm r}(2t)]^m\, e^{2i\phi_0 t} e^{-2i\phi t} dt \tag{13}$$

To exemplify the procedure, we modeled the magnetic fields in spiral galaxies as a mixture of regular fields and random fields in which the random field cells are placed at equal distances along the line of sight, and the regular field of constant strength fills the space between the cells. The thermal electron density is the same in and between the cells. We stress again that the polarized radio emission is entirely produced in the regions with regular field. We may call it "mix" model.

For m cells of the random field and $m+1$ segments of length s of the regular field fixed in the"mix" model, the integrated polarization is computed by

$$\begin{aligned}\frac{P(\lambda^2)}{p_i} &= \sum_{j=0}^{m} \left[g(2\lambda^2)\right]^j \int_{j(s+l_0)}^{(j+1)s+jl_0} \epsilon(x) e^{2i\phi_0(x-jl_0)\lambda^2} dx \\ &= \frac{\sin[\lambda^2\phi_0(s)]}{(m+1)\lambda^2\phi_0(s)} \sum_{j=0}^{m} \left[g(2\lambda^2)\right]^j e^{i\phi_0[(2j+1)s]\lambda^2}\end{aligned} \tag{14}$$

where the normalized emissivity $\epsilon(x)$ of regular field segments is assumed to be a constant $1/((m+1)s)$ in the last expression. $((m+1)s$ is the total extent of the regular field along the line of sight). No emission is assumed from the random field cells.

Fig. 3 gives variations of the fractional polarization and angle with λ^2 of the radio emission for a set of typical galactic parameters. The dashed curve represents the case of $m = 10$ which may correspond to observing a spiral galaxy face-on. The solid curve stands for the case of $m = 100$ which may correspond to a spiral galaxy seen edge-on. The locations of the minimum points are now determined by the total Faraday depth of the regular field. For any more complicated configurations of the magnetic field and emissivity distribution, the depolarization can be constructed from the above equation.

It is interesting to note that the polarization angle converges to 45° when $\lambda^2 \to \infty$. This can be understood as the real part of Eq. (14) approaches the imaginary part when λ^2 becomes large. The converging rate depends on the choice of physical parameters, the larger the ratio $B_{\rm R}/B_{\parallel}$, the faster the convergence.

2.4. Depolarization in a Kolmogorov-type random field

The energy density function of random fields which obey a Kolmogorov spectrum may be written as

$$W(k) \sim k^{-5/3}, \quad k_1 \le k \le k_2 \tag{15}$$

where k is the wave number on scale length l, i.e. $k = 1/l$. The energy density function can also be expressed in terms of l. Solving the equation $W(l)dl = W(k)dk$, we have

$$W(l) \sim l^{-1/3}, \quad l_1 \le l \le l_2 \tag{16}$$

derived from the relation $l \propto k^{-1}$. At energy equilibrium of magnetic field and turbulent motion of gas, the strength of the random magnetic field on scale l is related to l by

$$B_{\rm r}(l) \propto l^{1/3}, \quad B_{\rm r} \le B_2 \tag{17}$$

where B_2 is the field strength on the largest cell scale l_2.

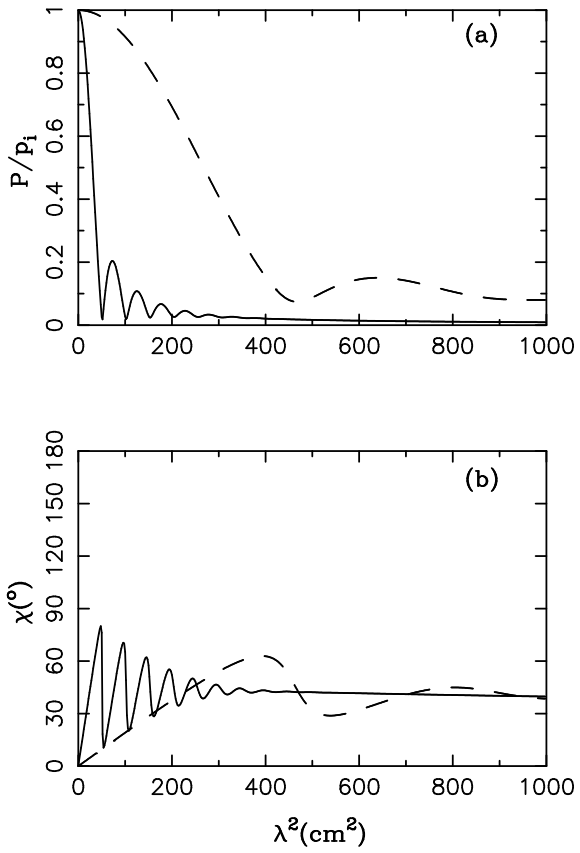

Fig. 3a and b. Depolarization of radio synchrotron emission in the "mix" model of regular and random galactic magnetic fields as a function of λ^2. The parameters are set to typical values: s = 50 pc, l_0 = 50 pc, n_e = 0.03 cm^{-3} inside and outside the cells, and $B_{\|} = B_R$ = 5 μG. The dashed curve is for the case m = 10 and the solid curve is m = 100. The emissivity has a constant form $\epsilon(x) = 1/((m+1)s)$. It should be noted that the total pathlengths are different for the two cases. **a** The fractional polarization; **b** the polarization angle.

The rotation measure produced by a cell of Kolmogorov-type random fields is given by

$$\psi = K n_e l B_r \cos\theta \tag{18}$$

where θ is the angle between the direction of the field B_r and the observer's line of sight where we fixed the thermal electron density n_e. A model with varying n_e and fixed B_r would give similar results.

Hence, ψ is a product of three random variables l, B_r and $\cos\theta$. The first two random variables l and B_r can be combined into one as $l^{4/3}$ by using Eq. (17), and the product has a distribution function

$$f(lB_r) \propto (lB_r)^{-1/2} \tag{19}$$

and its variation range is determined by those of l and B_r.

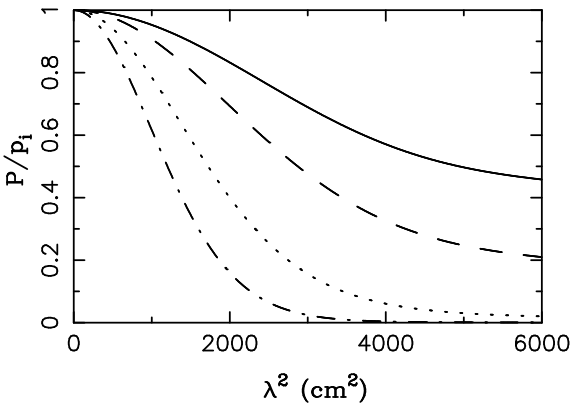

Fig. 4. Similar to Fig. 1 but with Kolmogorov-type random magnetic fields. The parameters of the largest cell scale are set to the typical values: l_2 = 50 pc, n_e = 0.03 cm^{-3} and B_2 = 5 μG. Different curves represent cases of a different number m of cells along the line of sight; the solid curve for m = 1; the dashed curve for m = 2, the dotted curve for m = 5 and the dashed-dotted curve for m = 10. Note that the polarization angle and rotation measure remains zero for all cases.

As demonstrated in Sect. 2.2, if the field orientation is assumed to be isotropic, then we have a normalized distribution of $\cos\theta$,

$$f(\cos\theta) = \frac{1}{2}, \quad -1 \le \cos\theta \le 1 \tag{20}$$

Therefore ψ virtually becomes a product of two random variables whose distributions are known. The distribution function of ψ is derived analytically as follows (see the Appendix for details)

$$f(\psi) = \frac{1}{2\psi_0^{1/2}}(|\psi|^{-1/2} - \psi_0^{-1/2}), \quad -\psi_0 \le \psi \le \psi_0 \tag{21}$$

where ψ_0 is the rotation measure produced by the largest cell scale of the random fields, $\psi_0 = K n_e B_2 l_2$. ψ has a mean $<\psi>$ = 0 and a variance $<\psi^2> = \psi_0^2/15$. We point out that this variance is significantly smaller than that given by the single-size cell model with $l_0 = l_2$ and $B_R = B_2$.

The characteristic function of $f(\psi)$ has only the real part

$$\begin{aligned} g(t) &= \int_{-\infty}^{\infty} [f(\psi)] e^{it\psi} d\psi \\ &= \int_0^1 (|z|^{-1/2} - 1)\cos(t\psi_0 z) dz \end{aligned} \tag{22}$$

and the integral can be evaluated numerically. The characteristic function of the Faraday dispersion function of m cells along the line of sight is just the m-fold of $g(t)$,

$$G_m(t) = [g(t)]^m \tag{23}$$

These functions are in fact the dispersion factors defined in Eq. (12).

The Faraday depolarization by one cell is just the characteristic function with the variable $2\lambda^2$, or the dispersion factor,

$$P(\lambda^2)/p_i = g(2\lambda^2) \tag{24}$$

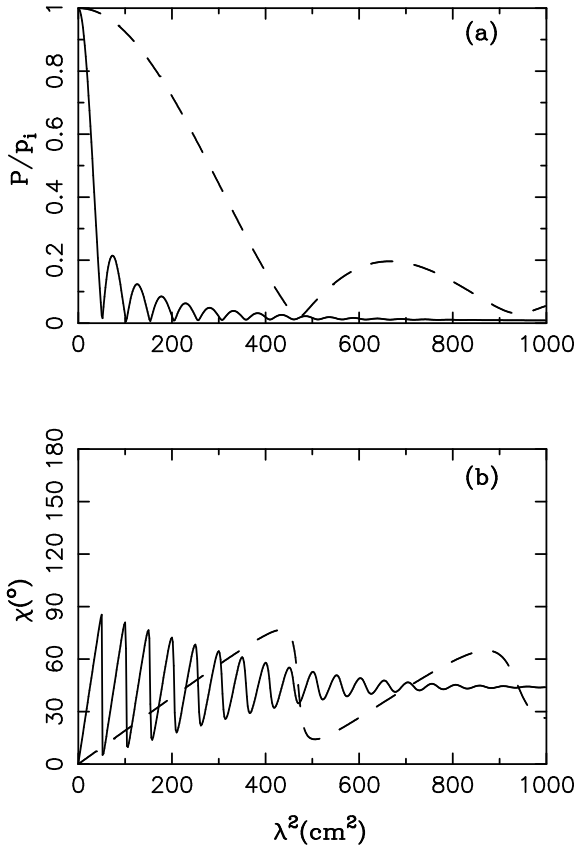

Fig. 5a and b. Similar to Fig. 3 (the "mix" model) but with Kolmogorov-type random fields. The parameters are set to typical values: $s = l_2 = 50$ pc, $B_{\|} = B_2 = 5\,\mu$G. The dashed curve is for $m = 10$ and the solid for $m = 100$. The emissivity has a constant form $\epsilon(x) = 1/((m+1)s)$. **a** The fractional polarization; **b** the polarization angle.

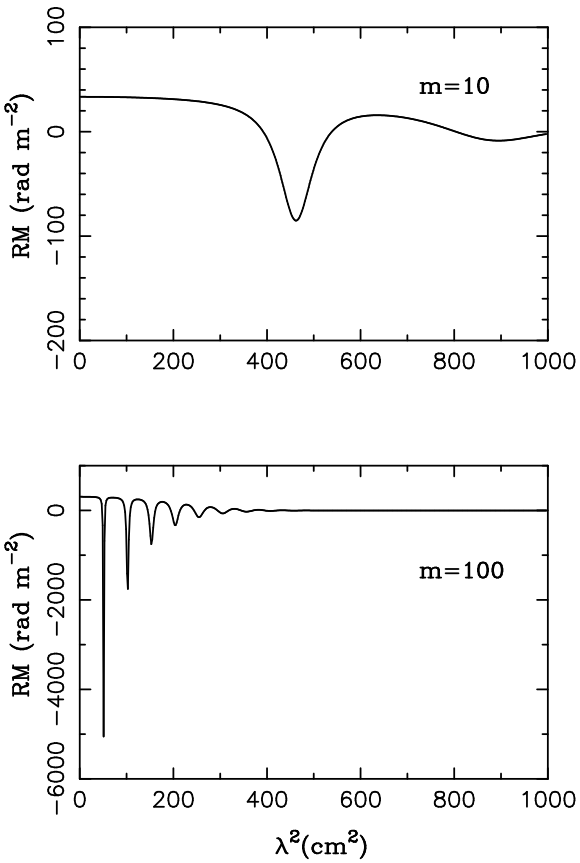

Fig. 6. Faraday rotation measures produced in the "mix" model with single-size random fields as a function of λ^2. The top curve is for $m = 10$ and the bottom one for $m = 100$. The parameters are the same as in Fig. 3.

For m cells, it is straight forward to write

$$P(\lambda^2)/p_{\rm i} = [g(2\lambda^2)]^m \tag{25}$$

The function $g(2\lambda^2)$ has only the real part which is always positive. Fig. 4 displays the polarization curves for a number of cells $m = 1, 2, 5, 10$, each with typical parameters $n_{\rm e} = 0.03\,{\rm cm}^{-3}$, $B_2 = 5\,\mu$G and $l_2 = 50$ pc. It clearly shows that the fractional polarization decreases monotonically with λ^2 and there is no zero point or local minimum. Again, as in Fig. 1, when m is very large, the fractional polarization will approach zero. In fact, Burn's (1966) Gaussian-type random field is the limiting case of our Kolmogorov type field.

Values of the fractional polarization for a given m are much larger in Fig. 4 than in Fig. 1. The reason is that the Faraday dispersion produced by the Kolmogorov-type random field is much smaller than that by the single-size cell random field if the largest cell of the Kolmogorov random field is set to be the same as the single-size cell random field. To explain the observed low values of fractional polarization by Faraday dispersion only, a large number of cells would be required, or larger values of l_2 or $n_{\rm e}$.

Now we incorporate the Kolmogorov type random fields into the "mix" model. The procedure is straight forward, just replacing the $G_{\rm m}$ in Eq. (7) with that defined in Eq. (23). Fig. 5 shows the results. The fractional polarization and angle vary in a similar way to those resulting from the single cell-size random field model as shown in Fig. 3. However, there is some difference between these two cases, and this will be discussed in the next Section.

2.5. Faraday rotation measures

In the presence of random fields with a significant strength and a finite size, the linear dependence of the polarization angle χ on wavelength λ^2 is severely distorted, as shown in Fig. 3b and Fig. 5b. Thus the commonly referred "rotation measure" RM is no longer a constant, but a function of λ^2. If one is still to keep its physical meaning, one has to generalize the definition of RM as

$$RM(\lambda^2) = \frac{d\chi(\lambda^2)}{d\lambda^2} \tag{26}$$

where χ is the polarization angle. The concrete form of RM will depend on the depolarization model. We calculated RM

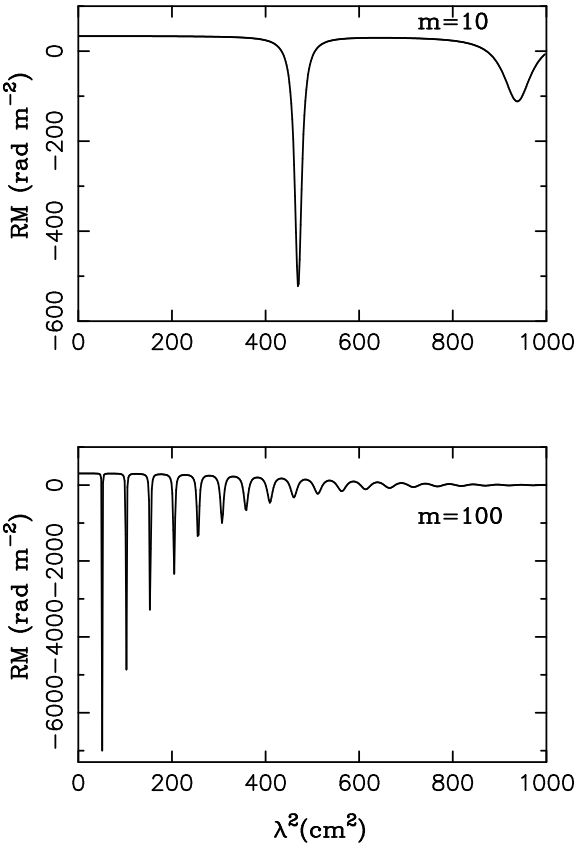

Fig. 7. Similar to Fig. 6 but with Kolmogorov-type random fields. The parameters are the same as in Fig. 5.

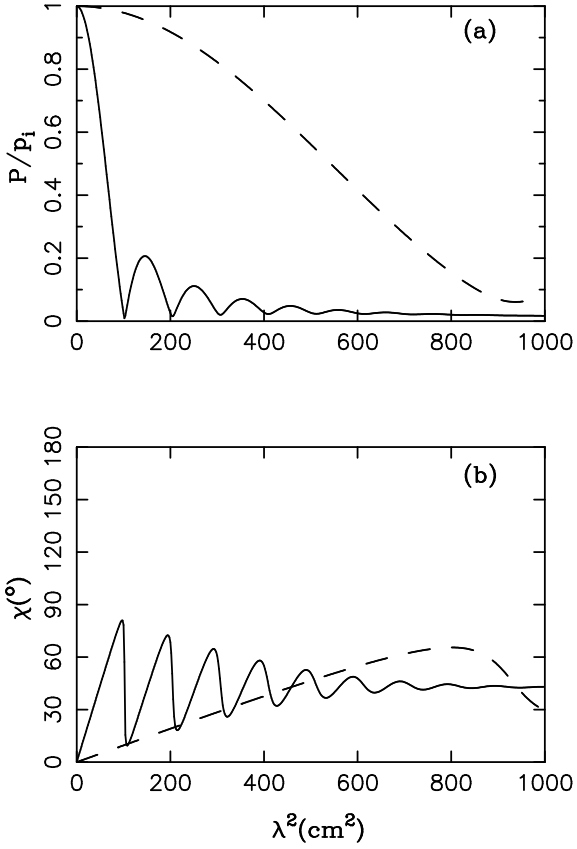

Fig. 8a and b. Similar to Fig. 5 but with different field strengths: $B_{\|} = 2.5\,\mu$G and $B_2 = 5\,\mu$G. **a** The fractional polarization; **b** the polarization angle.

as a function of λ^2 for the "mix" model described by Eq. (14). The results are shown in Fig. 6 and Fig. 7, which correspond to Fig. 3b and Fig. 5b, respectively.

RM is an oscillating function of λ^2 and its period is identical to that of the χ-variation. The RM amplitude is decreasing with increasing λ^2 and approaches zero when λ^2 is large enough. Comparing Figs. 6 and 7, the rate of decrease is determined by the magnitude of Faraday dispersion by the random fields. The single-size random fields have a larger effect than the Kolmogorov-type random fields. Another significant feature are large negative RM values near the minima of fractional polarization. Thus it should be noted that the occurrence of RMs of reversed sign does not require a reversal in the direction of the regular field.

3. Discussion and conclusions

As mentioned in the Introduction, there are a number of "anomalous" phenomena observed in radio polarization measurements which cannot be explained by the Burn's classical model. In this work we include the effect of finite-size cells of random fields. This formulation represents more realistic conditions in the interstellar medium because our "cells" can be identified as supernova remnants or large bubbles blown by stellar winds in a cluster of stars.

In Burn's slab model for regular magnetic fields, minima of the fractional polarization occur when the Faraday rotation angle reaches 90°. In our more realistic models, however, there is a slight shift between the minima of the fractional polarization and maxima of the angle (see Figs. 3 and 5), i.e. the phase of the angle oscillation is a little ahead of that of the fractional polarization, and the Faraday rotation measure is no longer constant with wavelength variation (Figs. 6 and 7). We attribute this effect to the existence of random fields. The details can be examined with help of Figs. 8 and 9. The strength of the regular field is halved in Fig. 8 and thus the random field strength is twice the regular one, while the other parameters remain unchanged. The 1σ width of the Faraday dispersion function becomes half of the Faraday rotation, so that the depolarization by Faraday dispersion of the random field cells becomes comparable to that by differential Faraday rotation of the regular field. The effect of the regular field is largely diluted and the phase correlation between the fractional polarization and angle is disappearing with increasing λ^2. However, the oscillation in the angle remains and its period is determined by the total Faraday depth of the regular field.

In Fig. 9, the strength of the random field is reduced by one half while the other parameters remain unchanged, so that the regular field dominates. The periodicity in the amplitude becomes more regular and the shift between the fractional polar-

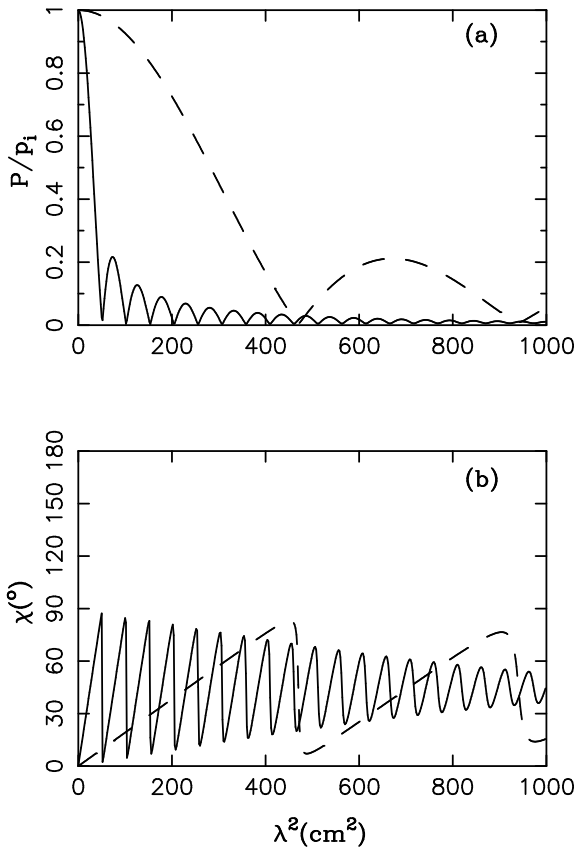

Fig. 9a and b. Similar to Fig. 5 but with different field strengths: $B_{\|} = 5\,\mu$G and $B_2 = 2.5\,\mu$G. **a** The fractional polarization; **b** the polarization angle.

ization and angle becomes smaller. Comparing with Fig. 5, it is clearly seen that the depolarization in Fig. 9 is mainly produced by the regular field.

We conclude that the effect of the random fields smears that of the regular field, and the amplitude of the oscillating fractional polarization is disappearing. A similar effect was already found by Burn (1966), but no details were given there. The lack of a correlation between DP and RM, as observed in a region of M31 (Berkhuijsen & Beck 1990), indicates that the random fields dominate. In this case, RM gradients across the telescope beam will also contribute to Faraday depolarization, but this effect is beyond the scope of this paper.

With the typical values of the parameters in our model, a galactic disk is "optically thick" for polarized radio emission at decimeter wavelengths. This is observed as a general decrease of rotation measure with increasing λ^2 (Beck 1993; Beck et al. 1996), as clearly visible in Figs. 6 and 7. If the depolarization by random fields dominates, the remaining polarized emission at decimeter wavelengths emerges from the nearest layer to the observer. The same is true in case of dominating depolarization by regular fields for wavelengths beyond the first zero point.

In the following, we will examine if the "anomalies" are due to the presence of finite-size cells of random field. The effect of the random fields is further demonstrated in Figs. 8 and 9 where we either increased or decreased the ratio of $B_{\rm R}/B_{\|}$ by a factor 2.

The cell size of the random fields in galactic halos is typically a few kpc (Dumke et al. 1995), so that the number of cells along the line of sight must be small. For $m \leq$10 we may expect to see significantly polarized emission at large (decimeter) wavelengths, in contrast to Burn's law $e^{-\lambda^4}$ (1966) which is valid only for an infinite number of cells. For the model in Fig. 5a, the fractional polarization at λ90 cm is 1.3%, and even larger in the other models of different sets of parameters (Figs. 3a, 8a, 9a). This may explain the detection of polarized emission around λ90 cm in our Milky Way Galaxy (Wieringa et al. 1993) and in the halo of the edge-on galaxy NGC 891 (Debreuck et al., in prep.).

Thus decimeter polarization may be a general phenomenon and should be searched for in other edge-on galaxies. Multi-frequency observations in the decimeter range could reveal the detailed variation of fractional polarization and Faraday rotation measure with wavelength and thus give constraints on the properties of the regular and random magnetic fields in galactic halos.

In the disks of spiral galaxies, regular and random fields have about equal strengths within a factor of 2 so that the situation in Figs. 3 or 5 (or in Figs. 8 or 9) applies. The periodicity in fractional polarization is less regular than that in Burn's slab model. The first minimum is no longer zero. The first harmonics of the fractional polarization show a period of $\Delta\lambda^2$ = 470 cm^2 for m = 10 which corresponds to the total Faraday depth of the regular magnetic field between the cells.

The observed "anomalous depolarization" in M51 (Horellou et al. 1992) can be easily understood. The wavelengths used (18 and 20 cm) are around a local minimum point in the curve of the fractional polarization (see e.g. Fig. 5a), so that a small variation in the magnetic field and/or in the thermal electron density will change the observed fractional polarizations and rotation measures dramatically, and no vertical magnetic fields are necessary. "Anomalous depolarization" ($DP = p(\lambda_2)/p(\lambda_1) > 1$ for $\lambda_2 > \lambda_1$) occurs if the observation wavelengths are located on an increasing branch of $p(\lambda^2)$ or on different sides of a minimum. The effect of "anomalous depolarization" is most prominent for a small number m of cells along the line of sight and for strong random fields (Fig. 8). Multi-frequency polarization observations of face-on galaxies are required for more detailed investigations.

The presence of large negative RM values occurring around minima of fractional polarization (Figs. 6 and 7) offer an alternative explanation for the "coronal hole" claimed to exist in the gas-rich, late-type spiral galaxy NGC 6946 (Beck 1991). The original interpretation was based on the detection of excess negative RMs (determined between λ18 cm and 20 cm) which were interpreted as vertical magnetic fields emerging from the disk. In view of the results presented in this paper, such negative values could well be an anomaly, visible in narrow ranges of Faraday depth values and invisible in other ranges, and are in fact not due to vertical fields. This has been verified by the non-detection of the excess of RM between 2.8 cm and 6.3 cm

wavelengths (Ehle & Beck 1993). Their map confirms that the internal Faraday depths are in the suitable range to generate zero points in fractional polarization and hence anomalously high RMs at $\lambda 20$ cm. Future observations with higher resolution will clarify why this phenomenon occurs only on the SW side of NGC 6946. Other mildly inclined, late-type spiral galaxies (e.g. M83, IC 342, NGC 2997) may show similar features if observed at a sufficiently high resolution.

RM values can be very small (either positive or negative) when λ^2 is large enough while magnetic field strengths and other parameters are kept fixed, as shown in Fig. 6 and Fig. 7. Equivalently, the same phenomenon occurs when the random magnetic fields become large enough while λ^2 and other parameters remain fixed. In radio galaxies, the magnetic field strength (both regular and random) is usually higher than that in normal spiral galaxies. In the observed wavelength range 6 cm − 20 cm, RM could well be small. This may explain the "anomalies" observed in 3C34 and 3C340 (Johnson et al. 1995) — the depolarization "silhouettes" are due to local enhancements of the random fields. A test for this hypothesis can be made by measurements of fractional polarization p and RM at shorter λ, say, at about 1 cm or even at millimeter wavelengths. If the observed p and RM are found to return to normal values, our explanation is supported.

In summary, polarization observations at radio wavelengths are suitable for studies of the structure of magnetic field in external galaxies. Our model successfully explains some of the observed "anomalous" phenomena. Multi-wavelength measurements are essential for reconstructing the variations of fractional polarization and polarization angle and thus for determining the important parameters of the magnetic field. Improved depolarization data will also show the accuracy of the Kolmogorov model for interstellar turbulence.

Appendix A: probability distribution of the product of two random variables

Let us define x and y to be two independent random variables with probability density functions

$$\begin{aligned} f(x) &\sim x^{-1/2},\ x_1 < x < x_2, \\ g(y) &\sim 1/2,\quad -1 < y < 1 \end{aligned} \tag{A1}$$

respectively. If we assume that $x_1 > 0$ and consider only the positive part of the y interval, we may take a logarithm transform of x and y,

$$\begin{aligned} u &= \ln x \\ v &= \ln y \end{aligned} \tag{A2}$$

and they have distribution functions of exponential form,

$$\begin{aligned} f(u) &\sim e^{u/2},\ u_1 < u < u_2 \\ g(v) &\sim e^{v},\quad -\infty < v < 0 \end{aligned} \tag{A3}$$

where $u_1 = \ln x_1$ and $u_2 = \ln x_2$.

Their characteristic functions are simply the Fourier transform, i.e.

$$\tilde{f}(t) = \int_{-\infty}^{\infty} f(u) e^{itu} du = \frac{e^{(it+1/2)u_2} - e^{(it+1/2)u_1}}{it + 1/2} \tag{A4}$$

Since it normally is held that $u_1 \ll u_2$ in our application, the above equation can be reduced to

$$\tilde{f}(t) = \frac{1}{it + 1/2} e^{(it+1/2)u_2} \tag{A5}$$

and

$$\tilde{g}(t) = \int_{-\infty}^{\infty} g(v) e^{itv} dv = \frac{1}{it + 1} \tag{A6}$$

Let w be the arithmetic sum of u and v, i.e.

$$w = u + v \tag{A7}$$

then the characteristic function of w is given by

$$\tilde{h}(t) = \tilde{f}\tilde{g} = \frac{1}{(it + 1/2)(it + 1)} e^{(it+1/2)u_2} \tag{A8}$$

The distribution function of w is the Fourier inverse of $\tilde{h}(t)$,

$$h(w) = \frac{1}{2\pi} \int_{-\infty}^{\infty} \tilde{h}(t) e^{-itw} dt \tag{A9}$$

This integral involves a complex variable and can be calculated using the residual theorem,

$$h(w) \sim e^{1/2} - e^{w - u_2/2}, \qquad \text{for } w \le u_2 \tag{A10}$$

Define the product of x and y to be $z = xy$, then we may write

$$z = e^{\ln x + \ln y} = e^{w} \tag{A11}$$

The distribution function of z can be derived from that of w,

$$H(z) = h(w)/z \sim z^{-1/2} - x_2^{-1/2}, \quad 0 < x \le x_2 \tag{A12}$$

From the consideration of symmetry, the distribution function over the negative interval is a miror of that in the positive. Therefore, the function over the whole interval may be written as

$$H(z) = C(|z|^{-1/2} - x_2^{-1/2}), \quad -x_2 \le x \le x_2 \tag{A13}$$

where $C = (2x_2^{1/2})^{-1}$ is the normalization factor.

Acknowledgements. The authors are grateful to Dr. E.M. Berkhuijsen for useful comments on the manuscript. The initial phase of this work was carried out at the Max-Planck Institute for Radio Astronomy, Bonn. X.C. wishes to thank Prof. R. Wielebinski for hospitality. R.B. is grateful to Drs. E.M. Berkhuijsen, M. Krause, A. Poezd and A. Shukurov for fruitful discussions on depolarization mechanisms. The referee, Dr. R.A.M. Walterbos, is kindly acknowledged for many useful comments.

References

Beck R., 1987. In: Beck R., Gräve R. (eds.) Interstellar Magnetic Fields. Springer-Verlag, Berlin, p. 2
Beck R., 1991, A&A 251, 15
Beck R., 1993. In: Krause F., Rädler K.-H., Rüdiger G. (eds.) The Cosmic Dynamo. Kluwer, Dordrecht, p. 283
Beck R., Brandenburg A., Moss D., Shukurov A., Sokoloff D., 1996, ARA&A 34, 155
Berkhuijsen E.M., Beck R., 1990. In: Beck R., Kronberg P.P., Wielebinski R. (eds.) Galactic and Intergalactic Magnetic Fields. Kluwer, Dordrecht, p. 201
Buczilowski U.R., Beck R., 1991, A&A 241, 47
Burch S.F., 1979, MNRAS 186, 519
Burn B.J., 1966, MNRAS 133, 67
Cioffi D.F., Jones T.W., 1980, AJ 85, 368
Cordes J.M., Weisberg J.M., Boriakoff V., 1985, ApJ 288, 221
Dumke M., Krause M., Wielebinski R., Klein U., 1995, A&A 302, 691
Ehle M., Beck R., 1993, A&A 273, 45
Feynman R.P., Hibbs A.R., 1965, Quantum Mechanics and Path Integrals. McGraw-Hill, New York
Horellou C., Beck R., Berkhuijsen E.M., Krause M., Klein U., 1992, A&A 265, 417
Johnson R.A., Leahy J.P., Garrington S.T., 1995, MNRAS 273, 877
Laing R.A., 1981, ApJ 248, 87
Le Roux E., 1961, Ann Ap 24, 71
Malofeev V.M., Shishov V.I., Sieber W., Jessner A., Kramer M., Wielebinski R., 1996, A&A, 308, 180
Rickett B.J., 1990, ARA&A 28, 561
Ruzmaikin A.A., Shukurov A.M., Sokoloff D.D., 1988, Magnetic Fields of Galaxies. Kluwer, Dordrecht
Spangler S.R., 1983, ApJ 271, L49
Tribble P.C., 1991, MNRAS 250, 726
Wielebinski R., Krause F., 1993, A&A Rev 4, 449
Wieringa M.H., de Bruyn A.G., Jansen D., Brouw W.N., Katgert P., 1993, A&A 268, 215

This article was processed by the author using Springer-Verlag LaTeX A&A style file *L-AA* version 3.